APEM journal

Advances in Production Engineering & Management
Volume 21 | Number 1 | March 2026 | pp 40–56
https://doi.org/10.14743/apem2026.1.560

ISSN 1854-6250
Journal home: apem-journal.org
Oroginal scientific paper

Optimization of a truck-autonomous unmanned vehicle distribution network with mobile charging and PV-storage integration

Liu, Y.H.[a,*], **Shi, X.L.**[a]

[a]School of Economics and Management, Beijing Jiaotong University, Beijing, P.R. China

ABSTRACT

This study investigates the collaborative optimization of routing and charging in a distribution network comprising electric trucks (ETs) and autonomous unmanned vehicles (AUVs), supported by mobile photovoltaic (PV) storage charging. A comprehensive optimization model is developed to minimize the total daily operating cost of the logistics enterprise, encompassing vehicle acquisition, staffing, energy consumption, charging, and penalties. The model simultaneously determines coordinated ET-AUV delivery routes, mobile charging schedules, and parking node locations. The PV-storage system is incorporated as a green power-supply constraint, directly influencing charging costs. To address the model's complexity, an enhanced hybrid frog-leaping algorithm is proposed. This algorithm incorporates an initial solution construction method to improve population quality, an advanced local deep search to increase search efficiency, and diversity control strategies with clone selection programs to maintain population diversity. The effectiveness of the developed algorithm is validated through multiple case studies with varying customer sizes. Computational experiments on instances with up to 60 customers indicate that, compared with the ET-only mode, the proposed ET-AUV collaborative mode reduces total daily operating costs by 18.61 %, decreases staffing costs by 62.5 %, and lowers penalty costs by 23.21 %, thereby enhancing customer satisfaction and operational resilience. Sensitivity analysis shows that system efficiency depends on several operational parameters. Increases in ET payload and range are the main drivers of cost reduction. Additionally, the average speeds of both vehicle types have a critical U-shaped effect on total costs.

ARTICLE INFO

Keywords:
Unmanned delivery;
Truck-autonomous unmanned vehicle routing optimization;
Mobile charging;
Photovoltaic storage charging;
Hybrid frog leaping algorithm;
Electric vehicle routing;
Energy-constrained routing

**Corresponding author:*
13811117792@126.com
(Liu, Y.H.)

Article history:
Received 12 December 2025
Revised 10 March 2026
Accepted 15 March 2026

1. Introduction

The rapid development of the Internet has accelerated the growth of online retail and e-commerce, creating substantial opportunities and demands for the logistics industry. However, these advancements have also introduced significant challenges, particularly regarding urban last-mile delivery. Increasing labour costs and restrictions on courier working hours impede logistics companies from providing efficient, stable, and nearly continuous distribution services, which places considerable pressure on fulfilment rates and cost management. Traditional delivery methods also increase physical contact between couriers and recipients, raising safety concerns, especially during public health emergencies. In densely populated areas such as campuses and residential complexes, truck access is frequently restricted. Moreover, as an energy-intensive sector, the logistics industry contributes significantly to greenhouse gas emissions. Population growth and urbanization have further intensified issues in urban distribution, including high energy consumption, extended delivery times, and

increased carbon emissions. In response to increasing distribution demand, rising customer expectations, worsening environmental pollution, growing urban traffic pressure, and other issues, innovative, high-quality, and automated distribution methods have become central to the competitiveness of the logistics industry during transformation and upgrading.

Within the evolution of intelligent logistics, unmanned delivery robots are emerging as a significant alternative to traditional delivery methods and are establishing a new business model in the modern logistics sector. In contrast to drones, autonomous unmanned vehicles (AUVs), although slower, are not constrained by low-altitude airspace regulations in urban areas, demonstrate greater adaptability to diverse weather conditions, and feature multiple compartments for distributing goods to various customers in a single trip. Furthermore, they generate substantially lower noise levels, making them more suitable for routine urban distributions [1]. Srinivas *et al*. [2] recently reviewed the literature on AUV routing and classified existing research into two categories: distribution modes relying solely on AUVs and those assisted by trucks, based on problem characteristics and application domains. Research on the former remains limited, primarily due to the inherent limitations of AUVs, such as reduced speed, limited range, and restricted payload [3]. Conversely, truck-assisted distribution modes present more advantages.

The truck-autonomous unmanned vehicle routing problem (TAUVRP) has become a significant focus of recent research. Based on system characteristics, TAUVRP is typically classified into two categories: the two-tier concept and the mothership concept [4]. In the two-tier concept, trucks operate at the first tier, transporting parcels from the warehouse to an AUV warehouse, which then delivers parcels to final customers at the second tier [5-7]. In the mothership concept, trucks are modified into mothership systems equipped with AUVs, traveling to various neighbourhoods and deploying AUVs to deliver parcels to nearby customers. Jennings and Figliozzi [8] and Simoni *et al*. [9] examine the mothership concept, focusing on scenarios where trucks do not wait at the same parking node for AUVs to return; however, neither study considers time window constraints. In contrast, Chen *et al*. [10] and Chen *et al*. [11] investigate a TAUVRP that incorporates time windows, requiring trucks to remain at the parking node until all dispatched AUVs have returned. Yu *et al*. [4] further categorize TAUVRPs based on whether trucks serve customers directly. In one type, trucks function as both mobile platforms for dispatching and collecting AUVs and as service providers to customers. In the other type, trucks serve solely as mobile platforms for dispatching and collecting AUVs. Building on this classification, Yu *et al*. [12] propose a TAUVRP that addresses simultaneous pickup and delivery. More recently, Mokhtari-Moghadam *et al*. [13] investigate the integrated optimization problem of AUV-drone collaborative distribution. In some cases, customer delivery demands may exceed the payload capacity of AUVs. If these demands are indivisible, serving such customers becomes infeasible. Therefore, incorporating multiple split deliveries by AUVs is essential for effectively addressing TAUVRP in urban environments.

Battery capacity limitations require AUVs to undergo multiple recharges during delivery trips, particularly when operating in truck-assisted modes. Most existing research on TAUVRP focuses on diesel trucks, with limited attention given to the use of electric trucks (ETs) and the charging of AUVs during transportation. Yu *et al*. [14] are among the few to address the optimization of ET-assisted distribution routes, utilizing ETs to provide on-board wireless charging for AUVs to improve delivery efficiency. To resolve ET charging challenges, various technologies such as fixed and mobile charging are employed to enhance convenience. Although fixed charging is the most prevalent, truck drivers may need to take detours to access charging stations, resulting in unnecessary power consumption. Additionally, long charging times can lead to queuing at stations, thereby reducing delivery efficiency [15]. To mitigate these issues, mobile charging vehicles (MCVs) can be deployed at strategic locations along ET routes, offering greater charging flexibility [16]. Integrated scheduling of ETs and MCVs is therefore essential for optimizing logistics and delivery systems. The decarbonisation of freight transportation through MCVs is also influenced by indirect carbon emissions associated with charging. If electricity is generated from thermal power, the widespread adoption of electric vehicles may undermine carbon reduction efforts. Consequently, research increasingly focuses on renewable energy charging facilities. Solar photovoltaic (PV) systems have been identified as a promising solution for enhancing the environmental benefits of logistics electrification [17]. Integrating PV systems, energy storage systems (ESS),

and charging piles effectively addresses the mismatch between PV generation and charging demand [18].

In summary, this study introduces MCVs, PV storage charging stations, and a multiple split distribution model to construct, for the first time, a truck-autonomous unmanned vehicle distribution network considering mobile photovoltaic storage charging (TAUVDN-MPSC). The contribution is threefold. First, for the TAUVDN-MPSC, a comprehensive optimization model is developed to simultaneously optimize ET-AUV distribution routes, mobile charging schedules, and parking-node locations while accounting for environmental, operational, and customer-service considerations. The objective is to minimize the sum of vehicle purchase cost, staffing cost, energy consumption cost, charging cost, and penalty cost. Secondly, given the complexity of the established model, an improved hybrid frog leaping algorithm (IHFLA) is proposed. This involves introducing an initial solution construction algorithm to enhance the quality of the population, developing an improved local deep search to improve local search efficiency, and incorporating diversity control strategies and clonal selection procedures to ensure population diversity. Finally, the performance of the IHFLA is validated using specially designed test cases of different scales. Sensitivity analysis is also applied to explore the impact of vehicle load and endurance mileage on the total operating cost. This is intended to provide key theoretical support and practical guidance for achieving a green, intelligent, and integrated urban logistics and distribution system.

2. Mathematical model

2.1 Problem statement

The TAUVDN-MPSC can be described as follows. Based on the actual urban distribution scenario, each ET carries AUVs and goods from the distribution centre and returns to the distribution centre after completing a daily distribution service, as shown in Fig. 1. ETs are not allowed to directly deliver goods to customers and must wait at the parking nodes to collect all AUVs they have dispatched before visiting the next parking node or returning to the distribution centre. Each parking node is visited by at most one ET. AUVs depart from the parking nodes to perform customer distribution services. Each customer has a soft time window $[e_i, l_i]$ and can only be visited by one AUV. Considering vehicle load constraints, this study assumes three AUV distribution modes: (1) single distribution, where the AUV completes a distribution service and returns to the parking node, then travels to the next location with the ET; (2) split distribution, where the same AUV makes multiple round trips to the parking node to provide distribution services to the same customer; (3) multiple distributions, where the same AUV makes multiple round trips to the same parking node to provide distribution services to different customers.

During the distribution operation, when the battery of an ET runs low, the distribution centre will arrange an MCV to charge it at the selected mobile charging node. After completing the charging, the MCV will proceed to the next mobile charging node or return to the distribution centre. The mobile charging node is selected from the unvisited parking nodes. It is assumed that the MCV arrives at the mobile charging node no later than the arrival time of the ET. ETs also serve as a mobile charging platform. When the AUV is mounted on the ET and travels to the next node, the AUV utilizes the time it spends on the ET to obtain electricity from the ET through wireless charging technology. In this way, energy flows from MCV to ET and then to AUVs, forming a complete chain supply. One MCV can charge multiple ETs, while each ET is only served by one MCV. The MCV carries a large battery and does not require recharging during service. A PV storage charging station is built at the distribution centre, where only PV output is generated on the generation side, providing charging for the MCVs, ETs, and AUVs parked at the distribution centre.

To standardize the description of mathematical models, a directed graph $G = (V, A)$ is given. The node set V includes a distribution centre V_0, a customer set V_c, a mobile charging node set V_{mc}, and a parking node set V_r. The arc set A includes an ET arc set A_1, an AUV arc set A_2, and an MCV arc set A_3. The ET set and the MCV set are denoted by K and M, respectively.

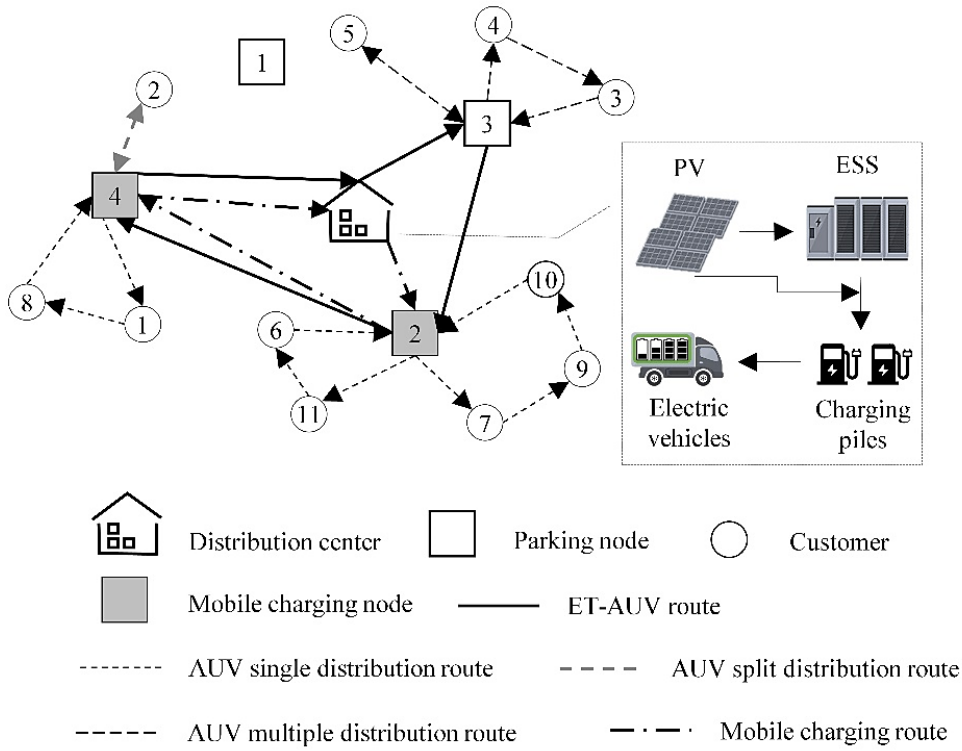

Fig. 1 Truck-unmanned vehicle distribution network

2.2 Symbol description

The settings and specific meanings of model decision variables and parameters are shown in Tables 1 and 2, respectively.

Table 1 Decision variables

Variables	Description
$x_{ij}^{AUV_k}$	1 indicates the AUV belonging to ET k passes arc (i,j), otherwise 0
y_j	1 means parking node j is selected, otherwise 0
z_j	1 indicates parking node j is selected as the mobile charging node, otherwise 0
$x_{ij}^{ET_k}$	1 indicates ET k passes arc (i,j), otherwise 0
$x_{ij}^{MCV_m}$	1 indicates MCV m passes arc (i,j), otherwise 0
$y_{j,mk}$	1 indicates MCV m at mobile charging node j provides charging services for ET k, otherwise 0

Table 2 Model parameters

Parameters	Description	Parameters	Description
pc_{AUV}	Cost of an AUV converted into one day	M_{MCV}	Unloaded mass of MCVs
sub_{AUV}	Cost of government subsidies equivalent to one day for AUVs	v_{ET}	Average running speed of ETs
pc_{ET_k}	The purchase price of an ET converted into one day	v_{MCV}	Average driving speed of MCVs
pc_{MCV_m}	One day purchase price of an MCV	v_{AUV}	Average driving speed of AUVs
c_{salary}	Average salary of a staff member	c_{mc}	Mobile charging price
c_w^{AUV}	Waiting time cost of AUVs	c_{PV}	PV charging price
c_d^{AUV}	Penalty time cost of AUVs	sub_{pv}	PV charging subsidy
$wt_i^{AUV_k}$	Early arrival time of AUVs	$pt_i^{AUV_k}$	Delay time of AUVs
$E_{d,j}^{ET_k}$	Battery power when ET leaves node j	C_{ET}	Maximum payload of ETs
c_w^{MCV}	Waiting time cost of MCVs	$at_i^{ET_k}$	Arrival time of ET

Table 2 (Continuation)

Parameters	Description	Parameters	Description
t_{ij}	Travel time along the arc (i,j)	st_i	Customer service time
$E_{a,j}^{ET_k}$	Battery power when ET arrives at node j	d_i	Customer demand
$E_{d,V_0}^{MCV_m}$	Battery power when MCV leaves V_0	C_{AUV}	Maximum payload of AUVs
$P_{ij}^{EV_k}$	Power demand of ETs passing through $(i,j) \in A_1$	Ψ	A large positive number
$P_{ij}^{AUV_k}$	Power demand of AUVs passing through $(i,j) \in A_2$	$at_j^{MCV_m}$	Arrival time of MCVs
P_{ij}^{MCV}	Power demand of MCVs passing through $(i,j) \in A_3$	E_{cap}^{AUV}	Battery capacity of AUVs
N_{AUV}^{max}	Maximum number of AUVs that can be carried by an ET	E_{cap}^{ET}	Battery capacity of ETs
$E_{d,j}^{AUV_k}$	Battery power when AUV leaves node i	E_{cap}^{MCV}	Battery capacity of MCVs
$E_{a,j}^{AUV_k}$	Battery power when AUV arrives at node i	λ	Regression coefficient
t_{full}^{ET}	Full charging time for ETs	ϕ	Battery efficiency
t_{full}^{MCV}	Full charging time for MCVs	g	Universal gravitation
e_{min}^{MCV}	Minimum remaining battery capacity of MCV	c_r	Rolling friction coefficient
e_{min}^{ET}	Minimum remaining battery capacity of ETs	c_d	Air drag coefficient
M_{ET}	Unloaded mass of ETs	ρ	Air density
$u_j^{ET_k}$	Load weight when ET arrives at j	f_s	Frontage
M_{AUV}	Unloaded mass of AUVs	α_{ij}	Slope
$N_{AUV}^{ET_k}$	Number of AUVs carried by an ET k	r_c	Charging efficiency
$u_j^{AUV_k}$	Load weight when AUV arrives at j	r_u	Utilization efficiency

2.3 Model formulation

The total operating cost of the logistics enterprise per day includes the vehicle purchase cost $C_{purchase}$, staffing cost C_{salary}, charging cost $C_{charging}$, energy consumption cost C_{cons}, and penalty cost $C_{penalty}$, as shown in Eq. 1. The vehicle purchase cost includes the purchase cost of pure electric trucks, driverless vehicles, and mobile charging vehicles, as shown in Eq. 2. Considering the government's subsidy and incentive policies for driverless vehicles, the purchase cost of driverless vehicles equals the procurement cost of driverless vehicles minus the government subsidies. The personnel cost is determined by the average salary of one logistics personnel and the required number of vehicles, as shown in Eq. 3. The calculation of charging cost is shown in Eq. 4, where the third term considers the waiting cost of mobile charging vehicles arriving at the mobile charging node ahead of schedule. In addition, the first term of Eq. 4 comprehensively considers the energy consumption of ET driving and the power consumption of ET for wireless charging of AUVs when calculating the total charging power provided by MCV, ensuring the balance and logical closure of the energy flow. Therefore, this mechanism is consistent with the mobile energy replenishment concept of MCV, but extends the charging level to end unmanned devices. Eq. 5 gives the energy consumption cost, where the energy consumption of pure electric trucks, driverless vehicles, and mobile charging vehicles during operation is shown in Eqs. 6 to 8, respectively. The penalty cost refers to the cost incurred when the driverless vehicle fails to meet the customer's time window during delivery, as shown in Eq. 9. For customers who require split delivery, the time window constraint is evaluated based on the start time of the first service for the customer.

$$min\, Z = min\left(C_{purchase} + C_{salary} + C_{charging} + C_{cons} + C_{penalty}\right) \tag{1}$$

$$\begin{aligned} C_{purchase} = &\sum_{k\in K}\sum_{j\in V_c}\left(pc_{ET_k} \times x_{V_0 j}^{ET_k} + (pc_{AUV} - sub_{AUV})N_{AUV}^{ET_k}\right) \\ &+ \sum_{m\in M}\sum_{j\in V_{mc}}\left(pc_{MCV_m} \times x_{V_0 j}^{MCV_m}\right) \end{aligned} \tag{2}$$

$$C_{salary} = c_{salary}\left(\sum_{k\in K}\sum_{j\in V_c} x_{V_0 j}^{ET_k} + \sum_{m\in M}\sum_{j\in V_{mc}} x_{V_0 j}^{MCV_m}\right) \tag{3}$$

$$C_{charging} = \sum_{j\in V_{mc}}\sum_{m\in M}\sum_{k\in K} z_j y_{j,mk} c_{mc}\left(E_{d,j}^{ET_k} - E_{a,j}^{ET_k}\right) + \sum_{m\in M}\left(c_{pv} - sub_{pv}\right)\left(E_{d,V_0}^{MCV_m} - E_{a,V_0}^{MCV_m}\right) + \sum_{m\in M}\sum_{j\in V_{mc}} z_j\left(c_w^{MCV} \times wt_j^{MCV_m}\right) \tag{4}$$

$$C_{cons} = c_{cons}\lambda\phi\left(\sum_{k\in K}\left(\sum_{(i,j)\in A_1} t_{ij}x_{ij}^{ET_k}P_{ij}^{ET_k} + \sum_{(i,j)\in A_2} t_{ij}x_{ij}^{AUV_k}P_{ij}^{AUV_k}\right) + \sum_{m\in M}\sum_{(i,j)\in A_3} t_{ij}x_{ij}^{MCV_m}P_{ij}^{MCV}\right) \tag{5}$$

$$P_{ij}^{ET_k} = v_{ET}\left(g\left(\sin(\alpha_{ij}) + c_r\cos(\alpha_{ij})\right)\left(M_{ET} + u_j^{ET_k} + N_{ADV}^{ET_k}M_{ADV}\right) + \frac{c_d\rho f_s {v_{ET}}^2}{2}\right) \tag{6}$$

$$P_{ij}^{AUV_k} = v_{AUV}\left(g\left(\sin(\alpha_{ij}) + c_r\cos(\alpha_{ij})\right)\left(M_{AUV} + u_j^{ADV_k}\right) + \frac{c_d\rho f_s {v_{AUV}}^2}{2}\right) \tag{7}$$

$$P_{ij}^{MCV} = v_{MCV}\left(gM_{MCV}\left(\sin(\alpha_{ij}) + c_r\cos(\alpha_{ij})\right) + \frac{c_d\rho f_s {v_{MCV}}^2}{2}\right) \tag{8}$$

$$C_{penalty} = \sum_{k\in K}\sum_{i\in V_c}\left(c_w^{AUV} \times wt_i^{AUV_k} + c_d^{AUV} \times pt_i^{AUV_k}\right) \tag{9}$$

s.t.

$$\sum_{(i,j)\in A_1} x_{ij}^{ET_k} = \sum_{(i,j)\in A_1} x_{ji}^{ET_k} \qquad \forall j \in V_c, k \in K \tag{10}$$

$$\sum_{(i,j)\in A_3} x_{ij}^{MCV_m} = \sum_{(i,j)\in A_3} x_{ji}^{MCV_m} \qquad \forall j \in V_{mc}, m \in M \tag{11}$$

$$\sum_{(i,j)\in A_2} x_{ij}^{AUV_k} = \sum_{(i,j)\in A_2} x_{ji}^{AUV_k} \qquad \forall j \in V_c, k \in K \tag{12}$$

$$x_{V_0 j}^{ET_k} = x_{iV_0'}^{ET_k} \le 1 \qquad \forall i, j \in V_c, k \in K \tag{13}$$

$$x_{ji}^{AUV_k} = x_{oj}^{AUV_k} \qquad \forall i, o \in V_c, j \in V_r, k \in K \tag{14}$$

$$\sum_{i\in V_c} x_{ji}^{AUV_k} \ge 1 \qquad \forall j \in V_r, k \in K \tag{15}$$

$$\sum_{k\in K}\sum_{j\in V_r} x_{ji}^{AUV_k} \ge 1 \qquad \forall i \in V_c \tag{16}$$

$$N_{ADV}^{ET_k} + u_j^{ET_k} < C_{ET} \qquad \forall j \in V_r, k \in K \tag{17}$$

$$u_j^{AUV_k} < C_{AUV} \qquad \forall j \in V_c, k \in K \tag{18}$$

$$N_{AUV}^{ET_k} \le N_{AUV}^{max} \qquad \forall k \in K \tag{19}$$

$$N_{AUV}^{ET_k} \le \max_{V_r}\left\{\sum_{j\in V_c} x_{V_r j}^{AUV_k}\right\} \qquad \forall k \in K \tag{20}$$

$$at_i^{ET_k} + \max\left\{st_i, \frac{z_i\left(E_{d,i}^{ET_k} - E_{a,i}^{ET_k}\right)}{r_c}\right\} + t_{ij} - at_j^{ET_k} \le \Psi\left(1 - x_{ij}^{ET_k}\right) \qquad \forall (i,j) \in A_1, i \in V_c, k \in K \tag{21}$$

$$at_i^{AUV_k} + wt_i^{AUV_k} + st_i + t_{ij} - pt_i^{AUV_k} - at_j^{AUV_k} \le \Psi\left(1 - x_{ij}^{AUV_k}\right) \qquad \forall (i,j) \in A_2, i \in V_c, k \in K \tag{22}$$

$$wt_i^{AUV_k} = max\left\{0, e_i - at_i^{AUV_k}\right\} \qquad \forall i \in V_c, k \in K \tag{23}$$

$$pt_i^{AUV_k} = max\left\{0, at_i^{AUV_k} - l_i\right\} \qquad \forall i \in V_c, k \in K \tag{24}$$

$$at_i^{MCV_m} \le at_i^{ET_k} + \Psi\left(1 - y_{i,mk}\right) \qquad \forall i \in V_{mc}, k \in K, m \in M \tag{25}$$

$$wt_j^{MCV_m} = max\left\{0, at_j^{ET_k} - at_j^{MCV_m}\right\} \qquad \forall j \in V_{mc}, k \in K, m \in M \tag{26}$$

$$at_i^{ET_k} + r_c\left(E_{d,i}^{ET_k} - E_{a,i}^{ET_k}\right) + t_{ij} \le at_j^{MCV_m} + \Psi\left(1 - x_{ij}^{MCV_m}\right) \qquad \forall (i,j) \in A_3, i \in V_{cm}, k \in K, m \in M \tag{27}$$

$$E_{cap}^{ET} = r_u \times t_{full}^{ET} \times r_c + e_{min}^{ET} \tag{28}$$

$$E_{cap}^{MCV} = r_u \times t_{full}^{MCV} \times r_c + e_{min}^{MCV} \tag{29}$$

$$0 < E_{a,j}^{AUV_k} \le E_{d,i}^{AUV_k} - P_{ij}^{AUV_k} t_{ij} x_{ij}^{AUV_k} + E_{cap}^{AUV}\left(1 - x_{ij}^{AUV_k}\right) \qquad \forall (i,j) \in A_2, k \in K \tag{30}$$

$$0 < E_{a,j}^{ET_k} \le E_{d,i}^{ET_k} - P_{ij}^{ET_k} t_{ij} x_{ij}^{ET_k} + E_{cap}^{ET}\left(1 - x_{ij}^{ET_k}\right) \qquad \forall (i,j) \in A_1, k \in K \tag{31}$$

$$0 < E_{a,j}^{MCV_m} \le E_{d,i}^{MCV_m} - P_{ij}^{MCV} t_{ij} x_{ij}^{MCV_m} + E_{cap}^{MCV}\left(1 - x_{ij}^{MCV_m}\right) \qquad \forall (i,j) \in A_3, m \in M \tag{32}$$

$$E_{d,j}^{AUV_k} \le E_{cap}^{AUV} \qquad \forall j \in V_r, k \in K \tag{33}$$

$$y_j \ge x_{ji}^{ET_k} \qquad \forall i \in V_r, k \in K \tag{34}$$

$$y_j = \sum_{(i,j)\in A_1} x_{ji}^{ET_k} \qquad \forall j \in V_r, k \in K \tag{35}$$

$$x_{ji}^{AUV_k} \le y_j \qquad \forall i \in V_c, k \in K \tag{36}$$

$$\sum_{i\in V_c} x_{ji}^{AUV_k} \ge y_j \qquad \forall j \in V_r, k \in K \tag{37}$$

$$z_j \le y_j \qquad \forall j \in V_r \tag{38}$$

$$y_{j,mk} \le z_j \qquad \forall j \in V_{mc}, m \in M, k \in K \tag{39}$$

$$z_j = \sum_{(i,j)\in A_3} x_{ij}^{MCV_m} \qquad \forall j \in V_{mc}, m \in M \tag{40}$$

Eqs. 10 to 12 represent flow balance constraints. Eq. 13 ensures that each ET is dispatched only once and returns to the distribution centre after completing its delivery task. Eq. 14 indicates that the AUV departs from the parking node and returns to the same node after completing its delivery. In addition, for a given AUV and parking node, when there is no split distribution or multiple distribution mode, Eq. 15 takes the value of 1; otherwise, Eq. 15 takes a value greater than 1. Eq. 16 indicates that each customer needs to be visited by an AUV and can be visited once or multiple

times, meaning that when there is a split distribution mode, customers will be served by AUVs multiple times. Eq. 17 limits the number of AUVs and goods carried by an ET to its payload. Eq. 18 limits the goods an AUV carries to its payload. Eqs. 19 and 20 state that the number of AUVs carried by an ET must not exceed either the maximum number of AUV journeys dispatched at all parking nodes or the specified maximum number of vehicles. Eqs. 21 and 22 represent time flow constraints for ETs and AUVs. Eqs. 23 and 24 are customer time window constraints. Eq. 25 ensures the MCV arrives at the mobile charging node no later than the ET. Eq. 26 gives the waiting time for the MCV. Eq. 27 provides a time flow constraint for the MCV. Eqs. 28 and 29 specify that all ETs and MCVs are fully charged when departing the distribution centre. Eq. 30 limits the travel distance of AUV and ensures its battery remains within capacity. According to Eq. 31, the energy of an ET arriving at node j cannot exceed its level when departing node i minus the consumption on arc $(i, j) \in A_1$. According to Eq. 32, the power level of an MCV when it reaches node j is not higher than the power level when it leaves node i minus the consumption through arc $(i, j) \in A_3$. The battery capacity will not exceed its limit at any time. If node i is the selected mobile charging node, subtract the electricity the MCV provides to the ET from the amount it has when leaving node i. Constraint 33 ensures that the battery state of the AUV is fully charged when it is first dispatched from its ET. In split distribution or multiple distribution modes, AUVs return to the ET and may depart again before being recharged, resulting in departures with less than maximum battery capacity. Eqs. 34 and 35 state that selecting a parking node requires ET visitation. Eqs. 36 and 37 are spatial coordination constraints for ETs and AUVs; that is, if parking node j is selected, it will serve at least one AUV dispatch activity. Eq. 38 limits charging node selection to chosen parking nodes. Eqs. 39 to 40 require that if an ET charges at a mobile charging node j, there must be a visiting MCV.

3. Solution approach

This study proposes IHFLA to address the TAUVDN-MPSC. The designed algorithm primarily consists of four stages: initial population construction, memeplex division, local deep search, and population shuffling, as illustrated in Fig. 2.

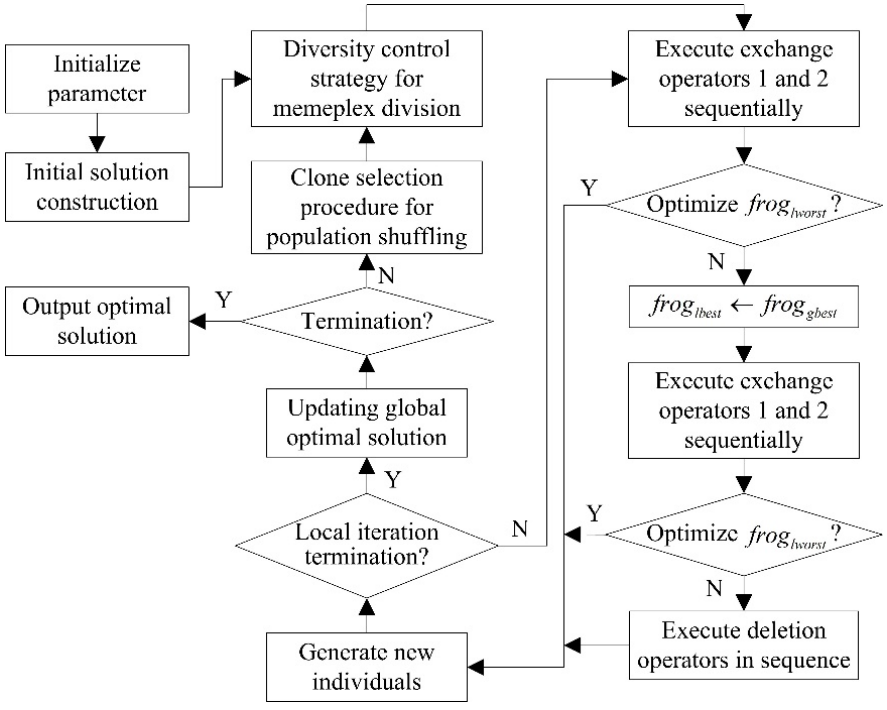

Fig. 2 Algorithm framework

The specific steps are as follows:

Step 1: Initial solution construction

Each individual represents a solution, encoded in three distinct parts (see Fig. 3). The first part specifies the routes of ETs. For example, ET 1 departs from distribution centre 0, visits parking nodes 3, 2, and 4 sequentially, then returns to 0. The second part details the routes of AUVs. For instance, AUV 1 initiates its route from parking node 3, returns to this node after serving customer 5, and subsequently serves customers 4 and 3 after reloading goods, before returning again to parking node 3. The third part outlines the routes of MCVs. For example, MCV 1 departs from distribution centre 0, charges the ET at parking nodes 2 and 4 in sequence, and finally returns to 0. Based on this encoding structure, the initial solution construction method is defined in steps 1-1 to 1-3, after which the generated initial solution is copied to N_{Pop}. Give $n_{Gen} = 1$.

Step 1-1: Initialize set $S_{AUV}^{dp} = \emptyset$, $V_r^{'} \leftarrow V_r$.

Step 1-1-1: Randomly select a customer as initial customer $c_{start} \in V_c$ and delete it.

Step 1-1-2: Randomly select $r_{dp} \in V_r^{'}$.

Step 1-1-3: If $d_{start} > C_{AUV}$, the AUV will go to and from the parking node $\left\lceil \frac{d_{start}}{C_{AUV}} \right\rceil$ times, and put the corresponding split distribution route $l_{AUV,s}^{new}$ in S_{AUV}^{dp}, return to step 1-1-1; If $d_{start} \leq C_{AUV}$, perform steps 1-1-4.

Step 1-1-4: If $V_c \neq \emptyset$, perform step 1-1-5; Otherwise, output S_{AUV}^{dp}.

Step 1-1-5: Select $c_{in} \in V_c$ to insert into the route of c_{start}. The best feasible insertion position is determined by Eq. 41.

If the range of AUV is violated after inserting c_{in}, it will not be inserted, and the current AUV route l_{AUV}^{cur} will be placed into S_{AUV}^{dp}. If $\left|S_{AUV}^{dp}\right| \geq N_{AUV}^{max}$, delete $r_{dp} \in V_r^{'}$ and return to step 1-1-1, otherwise directly return to step 1-1-1.

If the range of AUV is met after inserting c_{in}, but $d_{dp}^{now} \geq C_{ET}$ ($d_{dp}^{now}$is the sum of all customer demands connecting r_{dp}), it will not be inserted, and put l_{AUV}^{cur} into S_{AUV}^{dp}. If $\left|S_{AUV}^{dp}\right| \geq N_{AUV}^{max}$, delete $r_{dp} \in V_r^{'}$ and return to step 1-1-1, otherwise directly return to step 1-1-1.

If the range of AUV is met and $d_{dp}^{now} < C_{ET}$ after inserting c_{in}, but $d_{AUV}^{now} \geq C_{AUV}$ (d_{AUV}^{now} is the distribution demand of AUV after inserting c_{in}), insert r_{dp} before c_{in}, and check whether the range of AUV is met. If violated, c_{in} will not be inserted and put l_{AUV}^{cur} into S_{AUV}^{dp}. If $\left|S_{AUV}^{dp}\right| \geq N_{AUV}^{max}$, delete $r_{dp} \in V_r^{'}$and return to step 1-1-1, otherwise directly return to step 1-1-1. Otherwise, insert r_{dp} and c_{in} in turn, and delete $c_{in} \in V_c$, then put multiple delivery route $l_{AUV,m}^{new}$ in S_{AUV}^{dp}. If $\left|S_{AUV}^{dp}\right| \geq N_{AUV}^{max}$, delete $r_{dp} \in V_r^{'}$ and return to step 1-1-1, otherwise directly return to step 1-1-1. If $d_{AUV}^{now} < C_{AUV}$, insert c_{in}, delete $c_{in} \in V_c$, and return to step 1-1-4.

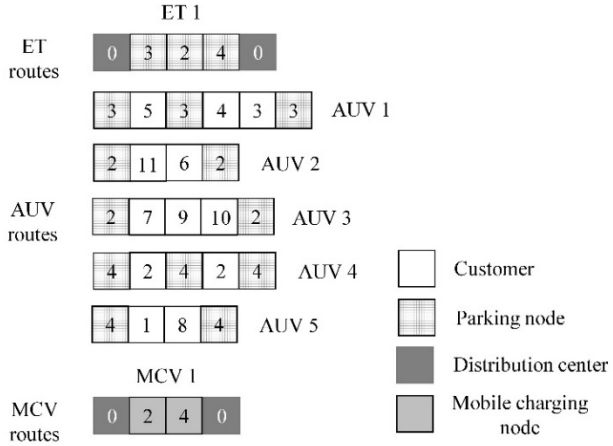

Fig. 3 Solution code representation

$$IC(i,c_{in},j)=\beta_1\left(t_{ic_{in}}+t_{c_{in}j}-\gamma t_{ij}\right)+\beta_2\left(at_{j,new}^{AUV_k}-at_j^{AUV_k}\right)+\beta_3\left(l_{c_{in}}-at_{c_{in}}^{AUV_k}\right) \quad (41)$$

where β_1, β_2 and β_3 are non-negative weight values and, $at_{j,new}^{AUV_k}$ is the new arrival time.

Step 1-2: Initialize set $S_{r,k}=\emptyset$, $V_{mc}=\emptyset$, and $T_{tw}=\emptyset$.
Step 1-2-1: Random select a parking node as the start parking node $r_{start}\in V_r$ and delete it.
Step 1-2-2: Initialize set $IV_r=\emptyset$. Store the remaining nodes of V_r into IV_r from small to large according to the distance to r_{start}.
Step 1-2-3: Traverse IV_r. If there is no parking node that meets the capacity limit of ETs after inserting, put the current ET route l_k^{cur} in $S_{r,k}$ and return to step 1-2-1. Otherwise, the selected parking node r_{dp} will be inserted between r_{start} and V_0, and delete it from V_r. Then, obtain a new ET route l_k^{new}.
Step 1-2-4: If the range of ET is violated, put r_{dp} into V_{mc}, and calculate the time of arrival and departure node r_{dp} as the time window, and put into T_{tw}
Step 1-2-5: If $V_r\neq\emptyset$, $r_{start}\leftarrow r_{dp}$, return to step 1-2-2; Otherwise, put l_k^{new}into $S_{r,k}$, and output, $S_{r,k}$, T_{tw} and V_{mc}.
Step 1-3: Initialize set $S_{mc}=\emptyset$.
Step 1-3-1: Randomly select a charging node as the starting charging point $s_{start}\in V_{mc}$ and delete it.
Step 1-3-2: Initialize set $IS_{mc}=\emptyset$. Store the remaining nodes of V_{mc} into IS_{mc} from small to large according to the distance to r_{start}.
Step 1-3-3: Traverse IS_{mc}. If there is no charging node that meets the available battery capacity of MCV after inserting, put the current MCV route l_k^{cur} into S_{mc}, and return to step 1-3-1;
Step 1-3-4： If it exist but does not meet Eq. 25, put l_k^{cur} into S_{mc} and return to step 1-3-1; Otherwise, insert the selected charging node s_{select} between s_{start} and V_0 to obtain a new MCV route l_k^{new}.
Step 1-3-5: If $V_{mc}\neq\emptyset$, return to step 1-3-2; Otherwise, put l_k^{new} into S_{mc}, and output S_{mc}.

Step 2: Memeplex division

The diversity control strategy [19] is used to divide the population N_{Pop} into N_M groups with the same size. First, the individuals are sorted according to the target value from small to large and stored in S_{Pop}. Then, the first N_M individuals in each group are taken as the first individual and deleted from S_{Pop}. After that, calculate the diversity values between the newly assigned individuals and the non-assigned individuals in S_{Pop}, and select the individuals with large diversity values to insert into the corresponding population. On this basis, memeplex groups are divided.

Step 3: Local deep search

Step 3-1: Determine global optimal individual $frog_{gbest}$ of the current population, and let $n_M=1$
Step 3-2: Select a memeplex M_j.
Step 3-3: Let $l=1$.
Step 3-4: Determine local optimal individual$frog_{lbest}$ and local worst individual$frog_{lworst}$ in M_j. Execute the exchange operators 1 and 2 in turn.

Exchange operator 1: Randomly select ET routes (l_k^{lbest} and l_k^{lworst}) from $frog_{lbest}$ and $frog_{lworst}$, respectively, and exchange them. Delete the duplicate customers in current $frog_{lworst}$, merge the distribution routes of the same parking node r_{same}, and judge whether the payload of ET is met. If not, delete the customers of r_{same} in the original $frog_{lworst}$ until the payload is met. Identify the unserved customers in $frog_{lworst}$ and insert back based on Eq. 41. If no feasible insertion location is found, a new distribution route is created and assigned to the nearest feasible parking node. Update the route number to generate a new individual $frog_{new}$.

Exchange operator 2: Randomly select parking nodes (r^{lbest} and r^{lworst}) from $frog_{lbest}$ and $frog_{lworst}$, respectively, and exchange them. Delete the duplicate customers in current $frog_{lworst}$, and check whether the payload of ET is met. If not, delete the customers served by other parking nodes until the payload is met. After that, the operation is the same as that in exchange operator 1.

Step 3-5: If $frog_{new}$ is not better than $frog_{lworst}$, $frog_{lbest} \leftarrow frog_{gbest}$, execute the exchange operators 1 and 2 in turn.
Step 3-6: If $frog_{new}$ is still not better than $frog_{lworst}$, execute the deletion operators for $frog_{lworst}$ in turn to generate $frog_{new}$.

Parking node deletion operator: Select the parking node with the least number of service customers and close it. Insert the deleted customer back based on Eq. 41. If no feasible insertion location is found, a new AUV route will be created and assigned to the nearest parking node.

Customer node deletion operator: Randomly select a customer and delete it. Insert this customer into other AUV routes based on Eq. 41. After that, the operation is the same as that in parking node deletion operator.
Step 3-7: Record $E_{a,r_{dp}}^{ET_k}$ and $E_{d,r_{dp}}^{ET_k}$ of ETs at each r_{dp}. If $E_{a,r_{dp}}^{ET_k} \leq 0$, the previous parking node of r_{dp} is selected as the mobile charging node, and then execute step 1-3 to optimize the MCV routes.
Step 3-8: If $l = L$, go to step 3-9. Otherwise let $l = l + 1$, return to step 3-4.
Step 3-9: If $n_M = N_M$, go to step 4. Otherwise let $n_M = n_M + 1$, return to step 3-2.

Step 4: Termination

If $n_{Gen} = n_{Gen}^{max}$, output the optimal solution. If $n_{Gen} < n_{Gen}^{max}$, go to step 5.

Step 5: Population shuffling

The clone selection procedure is used for population shuffling. First, the number of each cloned individual is calculated to generate a cloned population. Next, for each selected individual, first execute the parking node deletion operator, followed by the customer node deletion operator, based on the mutation probability. This sequence creates a new solution. Finally, use the roulette mechanism to select N_{Pop} individuals from the cloned population to form a new population, then return to step 2.

4. Results and discussion

4.1 Parameter condition setting

This study simulates a square urban area of $[0,30]^2$ km and divides it from inside to outside into Region 1 (city centre), Region 2 (surrounding area), Region 3 (suburban area), and Region 4 (external area). It is assumed that distribution centres are randomly distributed in Region 4, customers are evenly distributed in Regions 1, 2, and 3, and delivery points are evenly distributed in Region 2. Candidate delivery points are set as 1/5 of the number of customers. The number of customers is set to $|V_C| = \{20,30,40,50,60\}$, thus constructing 5 cases, namely Case 20-4, Case 30-6, Case 40-8, Case 50-10, and Case 60-12.

Due to the consideration of split distribution, 20 % of customer demands are evenly distributed within [5,30] kg, while the remaining customer demands are evenly distributed within [5,20] kg. The soft time window of customers is generated based on Solomon [20]. According to the average salary of on-duty employees in Beijing, the average salary of a logistics worker is 345 Yuan RMB/person·day. The range of the ET is set to 220 km, the battery capacity is 43 kWh, the driving speed is 40 km/h, and the self-weight is 1900 kg. The effective load is set to half of its payload, which is 600 kg. Its service life is assumed to be 10 years, so the purchase cost equivalent to one day is 35.56 Yuan RMB/vehicle·day. The minimum remaining battery capacity is equal to 20 % of the battery capacity. Taking Starship as an example, an ET can carry up to 6 AUVs. The maximum range of each AUV is 20 km, the driving speed is 10 km/h, the payload is 20 kg, the self-weight is 80 kg, and the charging rate is 5 kW. Its service life is assumed to be 5 years, so the purchase cost and subsidy converted into one day are 21.92 Yuan RMB/vehicle·day and 6.58 Yuan RMB/vehicle·day, respectively. The average service duration of ETs at parking nodes is set to 10 minutes. Additionally, the MCV is equipped with a battery capacity of 200 kWh, weighing 4500 kg and capable of a driving speed of 40 km/h. Its service life is assumed to be 10 years, so the purchase cost equivalent to one day is 164.38 Yuan RMB/vehicle·day. Currently, the cost of directly using PV generation to charge in China ranges from 0.40 to 0.70 Yuan RMB/kWh, while a subsidy of 0.03 to

0.05 Yuan RMB/kWh is provided. This study uses the median value, where the PV charging price is 0.55 Yuan RMB/kWh and the PV charging subsidy is 0.04 Yuan RMB/kWh. The mobile charging price is 0.77 Yuan RMB/kWh. For parameters related to energy consumption, refer to Demir *et al*. [21] and Goeke and Schneider [22]. For parameters related to algorithms, refer to Song *et al*. [23]. All experimental procedures are executed using MATLAB R2021a encoding.

4.2 Algorithm performance analysis

To evaluate the performance of IHFLA, this study compares IHFLA with the Genetic Algorithm (GA). In GA, individual selection is based on roulette wheel selection; crossover operation involves exchanging all AUV routes served by the same ET, and mutation operation targets individual customers for mutation. For each test case, both algorithms are run 10 times, and the optimal objective value Z_{best}^{IHFLA} (Z_{best}^{GA}), average objective value $\bar{Z}^{IHFLA}$ ($\bar{Z}^{GA}$), and average running time $\bar{t}^{IHFLA}$ ($\bar{t}^{GA}$) are recorded. Indicators Gap_1, Gap_2, and Gap_3 represent the differences in optimal objective value, average objective value, and average running time between the two algorithms, as shown in formulas (42) to (44). As shown in Table 3, the optimal objective values obtained by IHFLA in the five test cases are all lower than those obtained by GA, with an average of -5.60 % across all cases. In terms of average objective value, the average across all cases is -9.80 %, indicating that IHFLA significantly outperforms GA. The average running time of IHFLA is lower than that of GA in three cases; while in the remaining two cases, the value is below 5.00 %. However, the average across all cases is -5.87 %. Therefore, in most cases, the running speed of IHFLA is comparable to or even superior to that of GA. Overall, IHFLA exhibits better stability than GA.

$$Gap_1 = \frac{\left(Z_{best}^{IHFLA} - Z_{best}^{GA}\right)}{Z_{best}^{GA}} \times 100\ \% \tag{42}$$

$$Gap_2 = \frac{(\bar{Z}^{IHFLA} - \bar{Z}^{GA})}{\bar{Z}^{GA}} \times 100\ \% \tag{43}$$

$$Gap_3 = \frac{(\bar{t}^{IHFLA} - \bar{t}^{GA})}{\bar{t}^{GA}} \times 100\ \% \tag{44}$$

Table 3 Indicator analysis

Cases	Gap_1 (%)	Gap_2 (%)	Gap_3 (%)
Case 20-4	-0.85	-2.51	-16.71
Case 30-6	-7.67	-13.10	-12.42
Case 40-8	-8.77	-14.17	-9.10
Case 50-10	-4.96	-9.26	4.59
Case 60-12	-5.76	-9.97	4.31
Average	-5.60	-9.80	-5.87

Large-scale instances with 60 client nodes more accurately reflect real-world scenarios, as the solution space expands exponentially and leads to more frequent and complex constraint conflicts. This study examines the search behaviour and performance of the IHFLA in addressing such large-scale instances. Fig. 4 presents the total operating cost of the logistics enterprise per day as a function of the number of iterations. The horizontal axis represents the number of iterations, while the vertical axis indicates the total operating cost of the logistics enterprise per day. The convergence curve for IHFLA demonstrates a rapid reduction in the initial objective function value, with most optimization completed within approximately 150 iterations. Subsequently, the algorithm enters a fine search phase and stabilizes near the optimal value after about 200 iterations, resulting in a smooth curve and the lowest convergence platform. These results indicate that IHFLA achieves high-quality solutions with fewer iterations, effectively balancing exploration and exploitation in large-scale, complex optimization, thereby improving both search efficiency and solution quality.

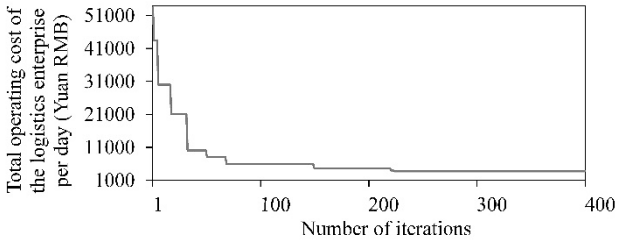

Fig. 4 Algorithm iteration convergence curve

4.3 Comparison of different distribution methods

This study presents a large-scale case involving 60 customers, comparing the traditional distribution method using only ETs with a transformed approach that incorporates both ETs and AUVs, as shown in Table 4. The ET-AUV distribution method reduces total operating costs by 18.61% and lowers penalty costs by 23.21%, indicating improved customer satisfaction and the ability to handle more complex distribution tasks. This innovation has led to changes in both fixed and variable costs. The traditional method requires six ETs, while the ET-AUV distribution method uses only two ETs, and AUVs do not require drivers, resulting in a 62.50 % reduction in staffing costs. In the traditional approach, ETs must visit all customers sequentially. In contrast, the ET-AUV distribution method allows multiple AUVs to be deployed from a parking node to serve nearby customers simultaneously, significantly reducing total distribution time. AUVs can use sidewalks or designated routes, are less affected by traffic congestion, and better meet customer time windows.

The number of ETs has been reduced from six to two. Despite this, the acquisition cost of six new AUVs is higher than the cost savings from reducing four ETs. This one-time investment is offset by significant savings in staffing and penalty costs during daily operations. The number of MCVs has been reduced from two to one. However, service targets have changed from six ETs to two ETs and six AUVs. This change increases total charging volume and charging costs. The distribution routes are longer, leading to increased total energy consumption. This results in a slight increase in energy consumption costs. Although vehicle purchase and charging costs rise with the ET-AUV distribution method, it still offers lower total operating costs, better human resource efficiency, and greater operational resilience than using only ETs.

Table 4 Comparison of optimization results under different distribution methods

Indicators	Only ET distribution method	ET-AUV distribution method
Total operating cost of the logistics enterprise per day (Yuan RMB)	4709.13	3832.58
Length of distribution routes (km)	127.60	137.67
Number of ETs (Vehicles)	6	2
Number of AUVs (Vehicles)	0	6
Number of MCVs (Vehicles)	2	1
Vehicle purchase cost (Yuan RMB)	542.12	1094.50
Staffing cost (Yuan RMB)	2760.00	1035.00
Charging cost (Yuan RMB)	355.46	639.99
Energy consumption cost (Yuan RMB)	787.02	859.96
Penalty cost (Yuan RMB)	264.52	203.13

4.4 Sensitivity analysis

This study is based on a large-scale calculation example involving 60 customers. It conducts sensitivity analysis of the payload and range, and runs IHFLA 10 times, recording the optimal solution. The results can provide appropriate operational decision-making references for practical operations.

Sensitivity analysis of payloads for ETs and AUVs

With other parameters remaining unchanged, this study analyses the impact of different payloads for ETs and AUVs on the total operating costs of the logistics enterprise per day. Sensitivity analysis is conducted by increasing or decreasing the baseline by 25% each time, as shown in Fig. 5.

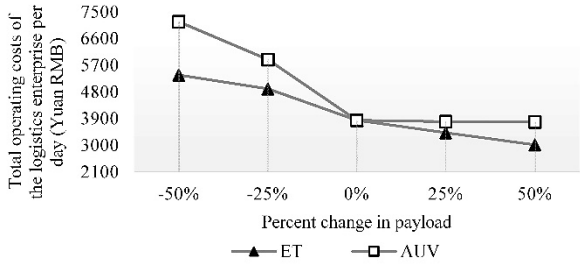

Fig. 5 Sensitivity analysis of payloads for ETs and AUVs

As the payload of ETs increases, the total operating costs show a downward trend. When the payload is too small (-50 %), the transport capacity of ETs is severely insufficient, requiring the deployment of more ETs to complete the same tasks, leading to increased staffing, energy consumption, charging, and vehicle purchase costs. When the payload increases by 25 % or more, the amount of cargo transported per trip increases, reducing the number of ETs required and spreading staffing and vehicle purchase costs. As the payload of AUV increases, the total operating costs show a trend of significant decrease followed by a slight increase. When the load is too small (-50 %), AUVs cannot effectively perform delivery tasks. It is necessary to deploy a large number of AUVs or make multiple round trips, leading to extremely complex scheduling, a surge in charging demand, and a large number of violations of time windows, ultimately resulting in a more than doubling of the total operating costs. When the payload increases by 25 % or more, the total operating costs remain almost unchanged, indicating that additional payload is redundant in most scenarios. In summary, as the most effective lever for reducing the total operating costs, ETs with greater payload should be preferred or deployed, subject to regulatory and road conditions. In contrast, when configuring the payload of AUVs, decision-makers should analyse the weight distribution of daily delivery orders and select a payload value that can cover the vast majority of order scenarios.

Sensitivity analysis of ranges for ETs and AUVs

Fig. 6 shows the impact of ETs and AUVs on the total operating costs of the logistics enterprise per day under different ranges. Similarly, sensitivity analysis is performed by increasing or decreasing the reference value by 25 % each time.

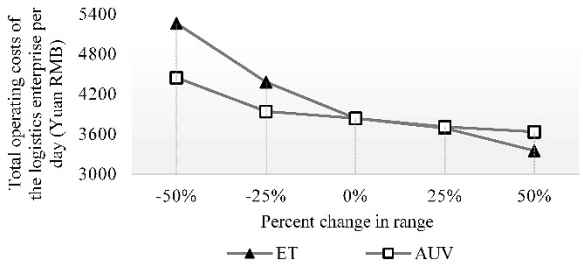

Fig. 6 Sensitivity analysis of ranges for ETs and AUVs

With the increase in the range of ETs, the total operating costs show a downward trend, and the penalty for the reduced range is far greater than the revenue from the increased range. When the range is too small (-50 %), ETs need to frequently and urgently call MCVs to charge in order to ensure daily distribution and operation, resulting in increased charging costs and charging waiting time. At the same time, due to the disruption of the distribution rhythm, the penalty cost for violating the time window surged. When the range increases slightly (+25 %), the endurance redundancy allows more flexible route planning, reduces the number of charges in the middle of a trip, and the total operating cost decreases slightly. With the further increase of the range of ETs, economies of scale have emerged, that is, a sufficient range may enable some vehicles to realize one-day charging, significantly reducing the dependence on mobile charging, and the costs of charging, vehicle purchase, staffing, and penalty have decreased significantly. With the increase

in the range of AUVs, the change in the total operating cost presents an L-shaped curve. That is, when the range increases by 25 % or more, the utility of additional range decreases, because a single delivery usually does not require such a long mileage, and the cost savings are minimal. However, when the range is significantly reduced (-50 %), the AUVs cannot effectively cover the customers around the parking node, and more AUVs need to be configured to meet the distribution demand, which greatly increases the charging time and scheduling complexity, resulting in an increase in energy consumption, charging, vehicle purchase, and penalty costs. To sum up, the range of ETs is the cornerstone to ensure the stability of the system. The cost savings from investing in a longer ET range are significant. The key to the range design of the AUV is to match the business scenario, which only needs to cover the distribution distance of most customers and leave a certain safety margin. Therefore, in the case of limited resources, priority should be given to ensuring the range of ETs.

Sensitivity analysis of average speed for ETs and AUVs

Holding all other parameter settings constant, this study examined the effects of varying average speeds of ETs and AUVs on the total operating costs of the logistics enterprise per day. Sensitivity analysis is performed by adjusting the benchmark speed by increments of 25 % above and below the baseline, as illustrated in Fig. 7.

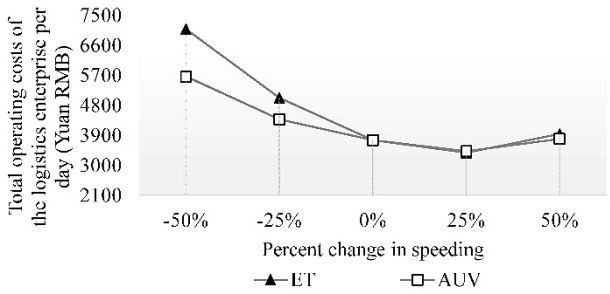

Fig. 7 Sensitivity analysis of average speed for ETs and AUVs

With the increase in the average speed of ETs, the total operating costs of the logistics enterprise per day show a U-shaped trend: it first decreases, then increases. When the speed is reduced by 50 %, the driving time doubles. This leads to two serious consequences. First, ETs arrive late at delivery nodes, causing batch delays in all AUV delivery tasks and sharply increasing time penalty costs. Second, prolonged driving time raises energy consumption per kilometre because of low motor efficiency, nearly doubling daily operating costs for logistics companies. When the average speed increases by 25 %, it approaches the economic speed. At this point, unit energy consumption drops to the optimal level, and punctuality is greatly improved. The penalty costs decrease significantly, making the total operating costs of the logistics enterprise per day reach their lowest point. If the average speed increases by 50 %, air resistance grows with the square of speed, causing a sharp rise in energy consumption costs. The potential to further reduce time penalty costs becomes very limited, leading to a rebound in total operating costs of the logistics enterprise per day. These patterns show that ETs have an optimal economic speed range. Decision-makers should keep the speed near this range to balance energy efficiency and punctuality. However, actual urban traffic conditions make truck speeds a random variable controlled by the environment, not something companies can fully manage. When traffic impacts are considered, the effect of speed changes on costs is even more pronounced.

With the rise in average speed of AUVs, the total operating costs of the logistics enterprise per day show a U-shaped trend. Costs first decrease, then increase, but the amount of fluctuation stays relatively small. When the average speed drops by 50 %, the delivery time becomes too long. This delay causes many customer services to fall outside the time window, sharply raising late penalty costs. Although energy use per mile is low at slower speeds, longer driving times increase auxiliary system energy consumption. This boosts charging costs and leads to a significant overall increase in total operating costs compared to the baseline. At 25 % higher average speed, vehicles

match customer time window requirements better, minimizing penalty costs. Although unit energy use rises, total operating costs decrease, reaching their best level. If speed increases by 50 %, air resistance sharply raises per-mile energy use. Early arrivals then cause new penalties, increasing total operating costs. This shows that the average speed needs flexible adjustment based on customer time window requirements. If the time window is loose, speed can drop to save energy consumption. If it is strict, speed should be moderately raised to ensure service. However, avoid excessive speed, which causes a rebound in energy use.

5. Conclusion

This study develops a comprehensive optimization model for an unmanned distribution system using ETs, AUVs, and MCVs to minimize the total operating costs of the logistics enterprise per day. The IHFLA algorithm developed to solve this model demonstrates significant advantages in both computational time and cost performance. Compared to the ET-only distribution, the ET-AUV distribution method offers lower total operating costs, improved human resource efficiency, and greater operational resilience. Sensitivity analysis indicates that the efficiency of the ET-AUV system depends largely on the core performance parameters. To reduce total operating costs, it is most effective to prioritize ETs with larger payloads, within the limits of laws, regulations, and road conditions. When resources are limited, enhancing the range of ETs should be the main focus. For AUVs, decision-makers should select payload and range values that meet most application needs, rather than maximizing these parameters unnecessarily. The average speeds of both ETs and AUVs have a U-shaped effect on total cost; therefore, ET speed should be kept within an economic range to balance energy consumption and punctuality, while AUV speed should be adjusted flexibly according to customer time windows to avoid higher costs caused by excessively low or high speeds.

In future research, we will consider soft time windows and resource-sharing mechanisms, allowing a parking node to be shared by multiple ETs over time or enabling multi-vehicle coordination through dynamic scheduling mechanisms, so that the model more closely reflects the complexity and variability of real-world distribution environments. The PV energy storage modelling will be expanded into a time-varying energy management system, considering factors such as sunshine intensity, energy storage status, and dynamic electricity prices, to achieve collaborative optimization of energy flow and logistics, making the model more closely aligned with actual operating scenarios. Moreover, future research will incorporate time-varying traffic and random fluctuations to simulate travel time uncertainty, as well as dynamic customer order arrivals and cancellations to create a dynamic demand scenario. Additionally, we will utilize Monte Carlo simulations and similar methods to evaluate the performance of the proposed model in stochastic environments, quantifying cost fluctuations and service failure rates under various disturbances. Further work will also explore dynamic rescheduling strategies and backup resource configurations, such as reserve AUVs, to strengthen the resilience of the system.

References

[1] Ghiani, G., Guerriero, E., Manni, E., Pareo, D. (2025). Combining autonomous delivery robots and traditional vehicles with public transportation infrastructure in last-mile distribution, *Computers & Industrial Engineering*, Vol. 203, Article No. 111001, doi: 10.1016/j.cie.2025.111001.

[2] Srinivas, S., Ramachandiran, S., Rajendran, S. (2022). Autonomous robot-driven deliveries: A review of recent developments and future directions, *Transportation Research Part E: Logistics and Transportation Review*, Vol. 165, Article No. 102834, doi: 10.1016/j.tre.2022.102834.

[3] Ulmer, M.W., Streng, S. (2019). Same-day delivery with pickup stations and autonomous vehicles, *Computers & Operations Research*, Vol. 108, 1-19, doi: 10.1016/j.cor.2019.03.017.

[4] Yu, S., Puchinger, J., Sun, S. (2020). Two-echelon urban deliveries using autonomous vehicles, *Transportation Research Part E: Logistics and Transportation Review*, Vol. 141, Article No. 102018, doi: 10.1016/j.tre.2020.102018.

[5] Campuzano, G., Lalla-Ruiz, E., Mes, M. (2025). The two-tier multi-depot vehicle routing problem with robot stations and time windows, *Engineering Applications of Artificial Intelligence*, Vol. 147, Article No. 110258, doi: 10.1016/j.engappai.2025.110258.

[6] Jin, Z., Lu, M., Li, X., Zhang, S., Hsu, S.C. (2025). Multi-objective optimization of two-echelon delivery with autonomous delivery vehicles and electric two-wheelers, *Computers & Industrial Engineering*, Vol. 203, Article No. 110999, doi: 10.1016/j.cie.2025.110999.
[7] Wei, Y., Wang, Y., Hu, X. (2025). The two-echelon truck-unmanned ground vehicle routing problem with time-dependent travel times, *Transportation Research Part E: Logistics and Transportation Review*, Vol. 194, Article No. 103954, doi: 10.1016/j.tre.2024.103954.
[8] Jennings, D., Figliozzi, M. (2019). Study of sidewalk autonomous delivery robots and their potential impacts on freight efficiency and travel, *Transportation Research Record: Journal of the Transportation Research Board,* Vol. 2673, No. 6, 317-326, doi: 10.1177/0361198119849398.
[9] Simoni, M.D., Kutanoglu, E., Claudel, C.G. (2020). Optimization and analysis of a robot-assisted last mile delivery system, *Transportation Research Part E: Logistics and Transportation Review*, Vol. 142, Article No. 102049, doi: 10.1016/j.tre.2020.102049.
[10] Chen, C., Demir, E., Huang, Y. (2021). An adaptive large neighborhood search heuristic for the vehicle routing problem with time windows and delivery robots, *European Journal of Operational Research*, Vol. 294, No. 3, 1164-1180, doi: 10.1016/j.ejor.2021.02.027.
[11] Chen, C., Demir, E., Huang, Y., Qiu, R. (2021). The adoption of self-driving delivery robots in last mile logistics, *Transportation Research Part E: Logistics and Transportation Review*, Vol. 146, Article No. 102214, doi: 10.1016/j.tre.2020.102214.
[12] Yu, S., Puchinger, J., Sun, S. (2022). Van-based robot hybrid pickup and delivery routing problem, *European Journal of Operational Research*, Vol. 298, No. 3, 894-914, doi: 10.1016/j.ejor.2021.06.009.
[13] Mokhtari-Moghadam, A., Salhi, A., Yang, X., Nguyen, T.T., Pourhejazy, P. (2025). A multi-objective approach for the integrated planning of drone and robot assisted truck operations in last-mile delivery, *Expert Systems with Applications*, Vol. 269, Article No. 126434, doi: 10.1016/j.eswa.2025.126434.
[14] Yu, S., Puchinger, J., Sun, S. (2024). Electric van-based robot deliveries with en-route charging, *European Journal of Operational Research*, Vol. 317, No. 3, 806-826, doi: 10.1016/j.ejor.2022.06.056.
[15] Yang, S., Zhang, R., Ma, Y., Zuo, X. (2025). Adaptive large neighborhood search incorporating mixed-integer linear programming for electric vehicle routing problem with mobile charging and nonlinear battery degradation, *Applied Soft Computing*, Vol. 175, Article No. 112988, doi: 10.1016/j.asoc.2025.112988.
[16] Çatay, B., Sadati, I. (2023). An improved matheuristic for solving the electric vehicle routing problem with time windows and synchronized mobile charging/battery swapping, *Computers & Operations Research*, Vol. 159, Article No. 106310, doi: 10.1016/j.cor.2023.106310.
[17] Calise, F., Fabozzi, S., Vanoli, L., Vicidomini, M. (2021). A sustainable mobility strategy based on electric vehicles and photovoltaic panels for shopping centers, *Sustainable Cities and Society*, Vol. 70, Article No. 102891, doi: 10.1016/j.scs.2021.102891.
[18] Wang, Y., Liu, X.Z. (2022). Day-ahead and intra-day two-stage optimal control of photovoltaic-energy storage charging station based on GRU-MPC, *Electric Power Automation Equipment*, Vol. 42, No. 10, 177-183, (in Chinese).
[19] Luo, J., Li, X., Chen, M.-R., Liu, H. (2015). A novel hybrid shuffled frog leaping algorithm for vehicle routing problem with time windows, *Information Sciences*, Vol. 316, 266-292, doi: 10.1016/j.ins.2015.04.001.
[20] Solomon, M.M. (1987). Algorithms for the vehicle routing and scheduling problems with time window constraints, *Operations Research*, Vol. 35, No. 2, 254-265, doi: 10.1287/opre.35.2.254.
[21] Demir, E., Bektaş, T., Laporte, G. (2011). A comparative analysis of several vehicle emission models for road freight transportation, *Transportation Research Part D: Transport and Environment*, Vol. 16, No. 5, 347-357, doi: 10.1016/j.trd.2011.01.011.
[22] Goeke, D., Schneider, M. (2015). Routing a mixed fleet of electric and conventional vehicles, *European Journal of Operational Research*, Vol. 245, No. 1, 81-99, doi: 10.1016/j.ejor.2015.01.049.
[23] Song, M.-X., Li, J.-Q., Han, Y.-Q., Han, Y.-Y., Liu, L.-L., Sun, Q. (2020). Metaheuristics for solving the vehicle routing problem with the time windows and energy consumption in cold chain logistics, *Applied Soft Computing*, Vol. 95, Article No. 106561, doi: 10.1016/j.asoc.2020.106561.